Electrochemically Modulated Complexation Process for Gas Removal and Concentration

Patricia A. Terry, H. Jeremy Walls, and Richard D. Noble
Dept. of Chemical Engineering, University of Colorado, Boulder, CO 80309

Carl A. Koval
Dept. of Chemistry and Biochemistry, University of Colorado, Boulder, CO 80309

An electrochemically modulated complexation process was designed to extract and concentrate a gas-phase solute. The process was based on flowthrough electrolysis cells that electrochemically modulate a liquid-phase mass-transfer agent between high and low solute affinity forms. The liquid phase in the high-affinity form contacts a feed gas phase for the extraction and contacts the receiving gas phase in the low-affinity form. The chemical system used to demonstrate the general process was a Cu(II)/Cu(I) redox couple in an acidic chloride electrolyte to both concentrate carbon monoxide against a pressure gradient and selectively separate it from a mixture with nitrogen. Experimental results and modeling of this process are reported. The kinetics of the electrolysis reactions in the flow cells are discussed within the context of rotating ring disk voltammetry experiments.

Introduction

Separation and concentration of gases into individual components is a critical issue in the chemical and environmental industries. In 1987 the National Research Council (NRC, 1987) targeted high-priority research needs and opportunities in chemical separations. Their report stated that the development of techniques that use agents or external fields to selectively remove solutes was a most promising area of research. Current gas-separation methods are energy intensive in terms of heat input duties. Because it is less expensive and more efficient than other alternatives, the use of electrical energy was suggested to minimize the energy requirement.

The addition of a regenerable and recyclable mass-separating agent that interacts with the species to be concentrated could enhance a gas separation. This technique, in fact, was also listed as a high-priority need by the National Research Council. In addition, conversion of electrical energy to chemical energy is quite efficient, making an electrochemical approach for concentration thermodynamically promising. These processes can be used for various chemical separations. Ward (1970) first demonstrated that by electrochemically cycling Fe(II) and Fe(III) within a liquid membrane, nitrogen oxide transport could be improved. Winneck (1990) has shown that an electric field can replace a pressure gradient in some gas separations. Jemaa et al. (1993) designed a continuous process to concentrate organonitrogen compounds by controlling the oxidation state of iron metalloporphryins in aqueous solution.

This research presents a combination of these methods to minimize the energy required in concentrating a gas. In this article, we report a continuous electrochemical process for regeneration of a mass-separating agent used to remove a gas from a feed phase and concentrate it into a receiving phase. The process employs hollow fiber membrane modules for phase contacting and flowthrough electrolysis cells for redox cycling of the mass-separating agent. The process is analyzed in terms of mass-transfer resistance in each of these elements. The principal objective of this research is to design and study a process that is capable of selectively removing a gas from one phase and concentrating it into another by electrochemically modulating a mass-separating agent. A copper(II,I)/aqueous HCl/KCl complexing system is used with carbon monoxide as a model solute/complexing agent system to demonstrate the general concepts. The system is characterized with respect to both mass-transfer and electrochemical cell efficiencies. A glassy carbon/platinum ring disk electrode is used to investigate the kinetics of the Cu(II,I)

Correspondence concerning this article should be addressed to R. D. Noble.

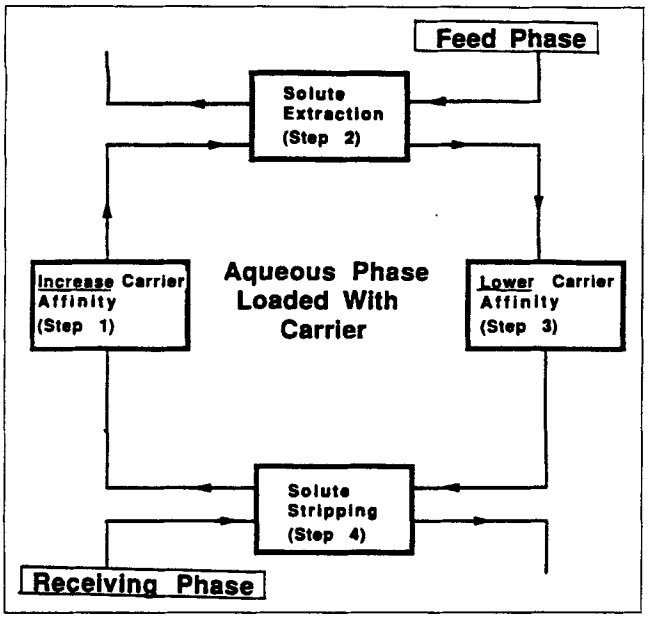

Figure 1. Separation/concentration process utilizing electrochemically modulated complexation.

redox couple and the potentials at which undesirable redox reactions occur. These results are discussed within the context of Cu(II,I)/CO complexation chemistry.

Process description

A diagram of an electrochemically modulated complexation (EMC) process is shown in Figure 1. The mass separating, or complexing, agent dissolved in the aqueous contacting phase is electrolyzed to its high solute affinity state in step 1. The solute is extracted from a feed gas phase by partitioning into the contact phase via reaction with the complexing agent in step 2. In step 3, the complexing agent is electrolyzed to its low solute affinity state. Following dissociation of the complex, the solute then partitions into the receiving gas phase in step 4. The contacting phase is then recycled.

The complexing agent must meet several requirements for an EMC process to be successful. First, it must be nonvolatile in the feed and receiving phases to prevent evaporative loss from the contacting phase. The complexing agent must have a solute binding site and must be able to undergo reversible oxidation and reduction, both in the presence and absence of solute. A considerable difference must exist between its affinities toward the solute in the two oxidation states. Solute is transferred by dissolving and binding to the complexing agent according to the following reactions:

$$C_{\text{red}} + P \overset{K_1}{\Leftrightarrow} C_{\text{red}}P$$

$$C_{\text{ox}} + P \overset{K_2}{\Leftrightarrow} C_{\text{ox}}P,$$

where C_{red} and C_{ox} are the complexing agent concentration in the reduced and oxidized forms; P is the free solute in solution; and K_1 and K_2 are the reaction equilibrium constants. Thus, K_1 must be significantly larger than K_2 for a considerable difference in affinities to exist. Lastly, the kinetics of the reactions of the solute with the complexing agent should be rapid enough to reach equilibrium in times that are short with respect to mass transfer.

We are investigating the use of water-soluble copper chlorides complex ions for removing carbon monoxide and other gaseous Lewis bases from a feed phase and concentrating them into a receiving phase. In an aqueous chloride solution, copper possesses the desirable characteristic of chemical reversibility between the cupric, Cu(II), and cuprous, Cu(I), states. The use of Cu(I) in chloride media for facilitated membrane transport of carbon monoxide has been reported by several groups (Smith and Quinn, 1980; Dindi, 1992). While copper chloride/carbon monoxide complexes are unstable in aqueous media, addition of acid to the system renders this a stable process. For the 1.0 M KCl and 0.1 M HCl electrolyte used in these studies, the reaction between Cu(I) and carbon monoxide is (Chaltykyan, 1966):

$$K_1 = 1{,}600\ \text{M}^{-1}$$

$$\text{Cu(Cl)}_3^{2-} + \text{CO} \Leftrightarrow \text{Cu(CO)(Cl)}_3^{2-}.$$

In this electrolyte, Cu(II) exists as a mixture of Cu^{2+}, $Cu(Cl)^+$ and $CuCl_2$ (McConnell and Davidson, 1950). These species have no appreciable affinity for CO, that is, K_2 is $\ll 1$. Because carbon monoxide has a high binding affinity in the reduced Cu(I) state and low affinity in the oxidized Cu(II) state, modulating the oxidation state of this copper complexing agent can significantly alter the degree to which the electrolyte solution absorbs CO.

Two distribution coefficients define the electrochemically modulated complexation process: K_r is the ratio of the solute concentration in the contacting phase to that in the feed phase when the complexing agent is in the reduced state; and K_o is the ratio of the contacting phase solute concentration to the receiving phase when the complexing agent is in the oxidized state. Both K_r and K_o are a function of the physical and chemical solubilities of the solute, the carrier concentration, and the degree of oxidation or reduction achieved in the flow cells.

A diagram of the experimental apparatus is presented in Figure 2. An aqueous copper(II) chloride solution is passed through two porous carbon flow electrodes to produce Cu(I). Carbon monoxide (solute) is extracted from a feed phase by binding with Cu(I) in a hollow fiber membrane module. The solute-rich contacting phase is then passed through a second pair of flow electrodes to produce the low affinity, Cu(II), form of the complexing agent. The dissociated solute is then concentrated in a receiving phase via contact in a second hollow fiber membrane module.

Experimental Section

Chemicals

Copper(II) and copper(I) chlorides (Mallinckrodt Specialty Chemicals and Sigma Chemical) dissolved in aqueous solution to a total concentration of 0.025 M in copper were used as the contacting solution. This solution also contained 1.0 M potassium chloride (Mallinckrodt) and 0.1 M hydrogen chloride (Mallinckrodt) as supporting electrolytes. Carbon

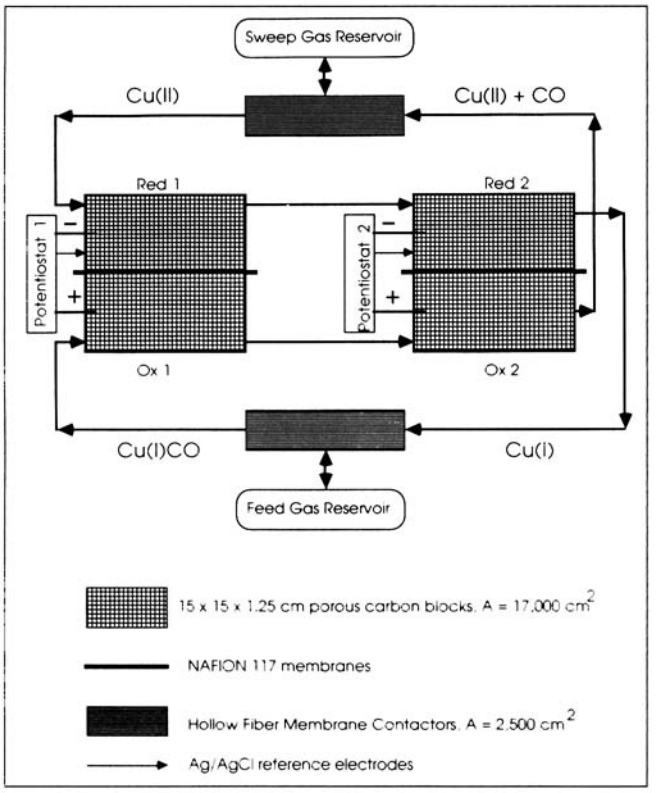

Figure 2. EMC process used to concentrate carbon monoxide.

monoxide (Specialty Products) was the feed and receiving phase, except for the mixture experiment where nitrogen (US Welding) was added.

Electrochemical flow cells

The design and operation of the electrochemical flow cells are one of the most important aspects of this work. Figure 2 shows a detailed view of the oxidation/reduction cycle through the electrodes. The flow electrodes behave as packed-bed chemical reactors. They are made by placing two porous carbon (Electrosynthesis Co.) block electrodes (15.25 cm × 15.25 cm × 1.25 cm) with a total surface area of 17,000 cm^3 inside a polyethylene shell. The two blocks, one used as the working electrode and the other as the counterelectrode, are separated by a sheet of Nafion 117 ion-exchange membrane to allow ionic conduction between them. Complexing agent reduction occurs at the working electrode and oxidation occurs at the counter electrode. Silver/silver chloride reference electrodes are placed near the flow inlet to the working electrodes. On the side opposite to the Nafion membrane, the blocks are pressure contacted with solid conducting graphite sheets that are connected to outside wire electrode contacts. Electrolysis potentials were applied using potentiostats that were constructed in house.

Hollow fiber membrane modules

The microporous polypropylene hollow fiber module (Hoechst Celanese) is composed of a large number of hydrophobic fibers placed in an outer shell similar to a shell-and-tube heat exchanger. The fibers have an internal diameter of 413 microns, a wall thickness of 30 microns, and 2,508 cm^2 of surface area. The Teflon shell is 3.0 cm in diameter and 20.5 cm in length. The membrane module offers the advantage of high contact area between the gas and liquid per unit volume. Because of the nondispersive nature of the contact, the two stream flows can be independently controlled. Due to the hydrophobicity of the fibers, the aqueous phase will not penetrate the fiber pores, allowing the gas to be transferred without mixing. The liquid/gas interface is immobilized at the fiber surface by keeping a higher pressure on the aqueous stream relative to the gas side.

Instrumentation

The concentrations of copper(II) in the aqueous solution were measured using a Hewlett-Packard HP8452A diode array UV-Visible spectrophotometer run with HP89531A MS-DOS UV/VIS operating software on a Zenith Z286 PC. For experiments involving a mixture of solvents, a Hewlett-Packard 5890 Series II gas chromatograph was employed with an HP 3396 Series II Integrator.

The rotating ring disk electrode (RRDE) studies were performed with a platinum/glassy carbon RRDE (Pine Instrument Co.) having a glassy carbon disk area $A = 0.41$ cm^2 and a collection efficiency $N = 0.18$. This electrode was polished prior to each use with 0.05 μm alumina. The values of A and N were determined experimentally using a 5.0-mM solution of $K_3Fe(CN)_6$ in 1.0 M KCl (Bard and Faulkner, 1980) and agreed well with dimensions provided by the manufacturer. The counterelectrode used was a Pt mesh and the reference electrode was an aqueous SCE. The potential of the SCE reference is approximately 40 mV positive of the Ag/AgCl reference used to control the flow electrodes. The RRDE experiments were performed using an RDE 3 bipotentiostat (Pine Instrument Co.) and X,Y,Y′ recorder.

Mathematical Model

Jemaa et al. (1992) analyzed electrochemically modulated equilibrium stage processes and developed a McCabe–Thiele graphical analog that estimates the required number of stages, the composition of each stage, and the equilibrium limits for both the feed and receiving phase concentrations. Although Jemaa derives the limits for a stage process, these limits also apply to continuous processes. These equilibrium limits, which are a function of the magnitude of the distribution coefficients, tell the maximum possible amount of solute that can be concentrated. As the ratio of K_r to K_o increases, greater concentration can be achieved from the feed to the receiving phase with fewer stages required.

The continuous EMC process is modeled by a mass-transfer mechanism that is a function of three resistances in the hollow fiber membrane contactors: flow outside the fibers, transfer across the hydrophobic membrane, and flow inside the fibers. In both modules, the aqueous solvent flows inside the fibers, while the solute gas flows in the shell.

Two overall mass-transfer coefficients, defined as K_{or} during the extraction step and K_w during the release step, are employed in the model. According to Prasad and Sirkar (1987), K_{or} for a hydrophobic membrane with the gas phase flowing outside the fibers can be described by

$$1/K_{or} = d_i[1/(d_o k_{of}) + 1/(d_{lm} k_m) + 1/(m d_i k_{wf})]. \quad (1)$$

For a hydrophobic membrane with the aqueous phase inside the fibers, as in the receiving module,

$$1/K_w = d_i[m/(d_o k_{of}) + m/(d_{lm} k_m) + 1/(d_i k_{wf})], \quad (2)$$

where m is K_r in the equation for K_{or} and K_o in the equation for K_w. The fiber inner, outer, and log-mean diameters are represented by d_i, d_o, and d_{lm}. The variables k_{of}, k_{wf}, and k_m are the mass-transfer coefficients for carbon monoxide in the gas phase, the liquid phase, and the membrane, respectively. They are each correlated functions of Sherwood, Schmidt, and Reynolds numbers. Again, according to Prasad and Sirkir, the mass-transfer coefficients inside and outside the fiber are expressed as:

$$Sh = 1.62\left(d_i^2 v_{aq}/lD_a\right)^{1/3} \quad \text{(inside)} \quad (3)$$

$$Sh = 5.9(d_e/l)(d_e v_f/\nu)^{0.6}(\nu/D_o)^{1/3} \quad \text{(outside)}, \quad (4)$$

where D_o and D_a are the diffusion coefficients for the solute in itself and in the aqueous solution, l is the fiber length, v_f and v_{aq} are the gas and aqueous solution velocities, d_e is the effective shell diameter, and ν is the kinematic viscosity of the solute.

This model is general and applies to both liquid extraction and gas absorption. Any chemical reaction effects are lumped with the mass-transfer coefficients. A mass balance on each gas reservoir and on each hollow fiber module yields the following set of equations:

$$\frac{C_f^1 - C_f^{1*}}{C_f^0 - C_f^{0*}} = \exp\left[\frac{4K_{or}l}{dv_f}\left(1 - \frac{Q_f}{K_r Q_a}\right)\right] \quad (5)$$

$$\frac{C_r^1 - C_r^{1*}}{C_r^0 - C_r^{0*}} = \exp\left[\frac{4K_w l}{dv_{aq}}\left(1 - \frac{K_o Q_a}{Q_r}\right)\right] \quad (6)$$

$$Q_a[C_a^1 - C_a^0(t-a)] = Q_f\left(C_f^1 - C_f^0\right) \quad (7)$$

$$Q_a[C_a^1(t-a) - C_a^0] = Q_r(C_r^1 - C_r^0) \quad (8)$$

$$V_f\frac{dC_f^1}{dt} = Q_f\left(C_f^0 - C_f^1\right) \quad (9)$$

$$V_r\frac{dC_r^0}{dt} = Q_r(C_r^1 - C_r^0). \quad (10)$$

The subscripts f, a, and r stand for the feed, aqueous, and receiving phases. The superscripts 0 and 1 stand for the entrance and exit of the modules. C^* denotes the feed or receiving phase concentration that would be in equilibrium with the aqueous-phase concentration. Velocities are denoted by v, and V denotes volume. The constant a is the time lag required for the aqueous phase to reach the second hollow fiber module after exiting the prior one.

A knowledge of the magnitude of the distribution coefficients is needed to evaluate the overall mass-transfer coefficients. All other parameters are measurable. This set of equations is solved numerically for the concentrations of the feed and receiving reservoirs as a function of time. The main variables of interest are the solute concentrations in the gas-phase reservoirs.

Results and Discussion

Flow electrode performance

Each of the oxidized and reduced solutions flow through both electrodes in cocurrent series (Figure 2). The rate of electrochemical reaction, expressed as the cell current, in each of the flow cells is controlled independently via the potentials applied by the individual potentiostats. The flow rate of Cu(II) or Cu(I) through the cells can also be expressed as a current using Faraday's law. The electrode efficiency, defined as the rate of electrochemical reduction of Cu(II) (or the rate of oxidation of Cu(I)) divided by the flow rate of Cu(II) (or rate of Cu(I) flow) through the electrode, is a function of aqueous flow rate. Figure 3 shows the measured cell current, which is the sum from the two cells, and the total current required for 100% efficiency as a function of flow rate. At low flow rates, the cell current increases linearly and the efficiency is high; however, as the flow rate increases, the current delivered to the flow cells begins to reach an asymptote and efficiency decreases. At this applied potential, the limiting current is approximately 1.3 A. According to the manufacturer's specifications, each porous carbon electrode is expected to have a surface area of approximately 17,000 cm^2. This implied that the average limiting current density for the two electrodes in series is only 3.8×10^{-5} A cm^2, an extremely low value.

Selection of the potentiostat operating conditions is critical to the performance of an experiment. Attempts to increase the cell currents by increasing the applied cell potentials resulted in deposition of copper metal at the cathode and, in

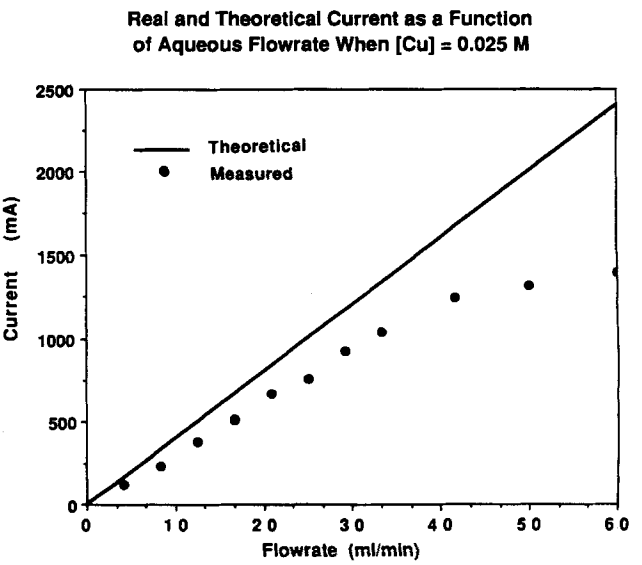

Figure 3. Electrochemical cell conversion as a function of the percentage of total current from electrode 1.

The working electrode potential for each flow electrode was −0.1 V vs. the Ag/AgCl reference.

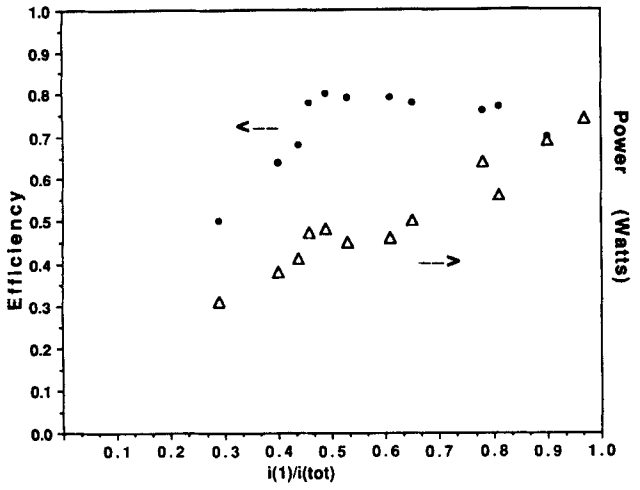

Figure 4. Electrolysis efficiency (left axis) and total power requirements (right axis) in the electrochemical cells as a function of the fraction of the current supplied by electrode 1.

Efficiency and power are defined in the text. The flow rate of the aqueous solution was 21 mL/min.

some cases, in the production of chlorine gas at the anode. Either of these occurrences reduces the capacity of the aqueous phase for the solute. Evolution of chlorine gas presents a possible safety hazard and could introduce errors in the pressure readings. The low current densities and undesirable side reactions observed in these cells are addressed below by the RRDE studies.

Current distribution between the two cells also affects the overall flow cell performance. Figure 4 shows both cell efficiency and power usage as a function of the fraction of total cell current provided by the first electrode. Power use was measured as the sum of the product of current and potential between the working and counterelectrodes for each cell. Efficiency reached a maximum between 0.4 and 0.6 current fraction. Power usage, on the other hand, increased almost linearly with increasing current fraction. These measurements indicated that the flow cells are best operated between 0.4 and 0.6 current fraction to obtain high conversion with the lowest possible power consumption.

Mass-transfer performance

Operation of the hollow fiber membrane modules is key to the mass-transfer rate of carbon monoxide from the feed to the receiving phase. Mass transfer in the membrane modules is affected by the flow configuration and both gas and aqueous flow rates. Comparison of mass-transfer resistances in the feed-phase module indicated that diffusion of gas through the aqueous solution to complex with Cu(I) was the limiting resistance and accounted for over 99% of the total. This resistance was minimized under conditions where aqueous solution flowed through the membrane fibers, thus minimizing the diffusion path to the fiber radius. Table 1 presents a comparison of initial gas-transfer rate in the feed membrane module as a function of aqueous flow rate. Increasing the flow rate raised the initial mass transfer until the point where the liquid residence time was too brief for efficient gas/liquid mixing. Above this limiting flow rate, mass transfer was significantly diminished. Due to mass-transfer limitations of the hollow fiber membrane modules, at no time was the physical solubility of the gas exceeded.

Table 1. Mass-Transfer Characterization

Aqueous Flow Rate mL/min	Initial Rate atm/min
13	0.010
21	0.027
34	0.031
47	0.043
78	0.040

EMC concentration of carbon monoxide

The extraction and concentration of carbon monoxide was performed according to the procedure described earlier. Figure 5 depicts the experimental and model results for a typical experiment. Carbon monoxide pressure decreased on the feed side from 1.01 atm to 0.16 atm and increased on the receiving side from 0.83 atm to 1.13 atm. Thus, carbon monoxide was concentrated between a maximum value of 0.16 and 1.13 atm, which is the difference that could be maintained if gas was continuously fed to one side and removed from the opposite side.

The equilibrium limits of 0.16 on the feed side and 1.13 atm on the receiving side indicate that the process achieved its maximum separation capability. The slope of the feed and receiving curves in Figure 5 represent the amount of gas that can be pumped per time at a given gas pressure difference. The absolute value of either slope decreases with time. On the feed side this is explained by the decreasing pressure,

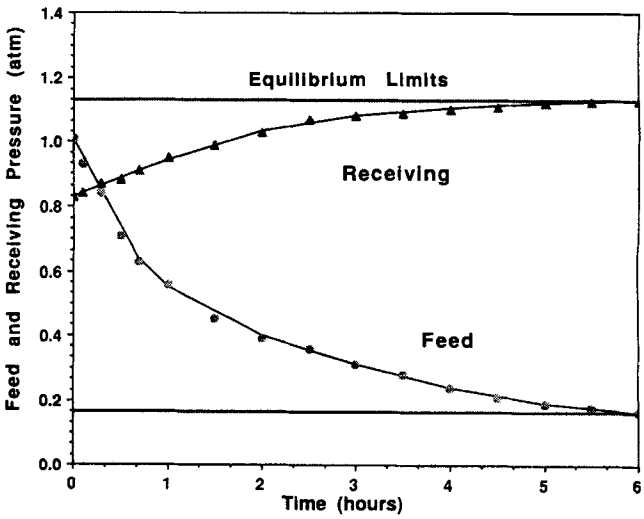

Figure 5. Carbon monoxide pressures in the feed and receiving cylinders during an EMC process.

Electrochemical cell current efficiency = 0.91, $[Cu]_{total}$ = 0.025 M, aqueous flow rate = 19 mL/min. Circles represent the feed cylinder pressure; triangles represent the receiving cylinder pressure. Solid lines through the data represent the calculation based on the mathematical model for this process (see text). The solid horizontal lines represent the calculated equilibrium limits.

Table 2. Separation of CO from Nitrogen

	Feed Pres. atm	Receiv. Pres. atm
Initial		
CO	0.61	0.81
N_2	0.44	0.03
Final		
CO	0.07	1.24
N_2	0.40	0.04

Flow rate = 27 mL/min; [Cu] = 0.025 M; Eff. = 0.95.

which reduces the solubility of the gas in the aqueous phase. In turn, the increasing pressure in the receiving phase causes the solubility to rise over time until the two solubilities are equal, where mass transfer ceases.

EMC concentration of CO in the presence of N_2

Due to the chemical selectivity provided by the carrier, EMC processes have the capability to separate a given solute from a mixture as well as to concentrate the solute. In order to demonstrate this concept, the extraction and concentration of carbon monoxide from a feed mixture with nitrogen was also performed using the EMC apparatus. Table 2 shows the initial and final CO and N_2 pressures in the feed and receiving reservoirs. The experimental conditions were aqueous flow rate of 27 mL/min, electrochemical cell efficiency of 95%. The time required to achieve the final pressures was approximately 2.5 h. An initial feed mixture of 0.61 atm CO and 0.44 atm N_2 and a receiving mixture of 0.81 atm CO with 0.03 atm N_2 were concentrated into a final feed mixture of 0.07 atm CO with 0.40 atm N_2 and a receiving mixture with 1.24 atm CO and 0.04 atm N_2. The CO concentration fraction in the feed phase was reduced from 0.58 to less than 0.16 and concentrated into a receiving mixture of 0.97 CO. Thus, CO was both selectively separated from a mixture with N_2 and concentrated into a receiving phase.

Rotating ring/disk electrochemical studies

In order to gain insight into the processes occurring in the flow electrolysis cells, RRDE studies were performed. The disk material was polished glassy carbon that would be expected to display electrochemical properties similar to the porous carbon used in the flow cells. The ring electrode is used to examine the reversibility of the processes occurring at the disk (Bard and Faulkner, 1980). Solutions composed of 0.025 M $CuCl_2$, 0.025 M CuCl, and 0.0125 M $CuCl_2$ and 0.025 M CuCl (all in 1.0 M KCl, 0.1 M HCl supporting electrolyte) were examined under argon and carbon monoxide atmospheres. These solution compositions represent the aqueous phases entering the cathode and anode compartments of the flow cells as well as a partially electrolyzed solution that exists between the two cells. The effect of mass transfer to the disk electrode was examined by varying the rotation rate between 100 and 4,000 rpm.

Figure 6 contains disk voltammograms for solutions containing Cu(II) and Cu(I) under Ar(top) and CO(bottom) atmospheres. In both cases, the oxidation process is found to be far more facile than the reduction process. By noting that

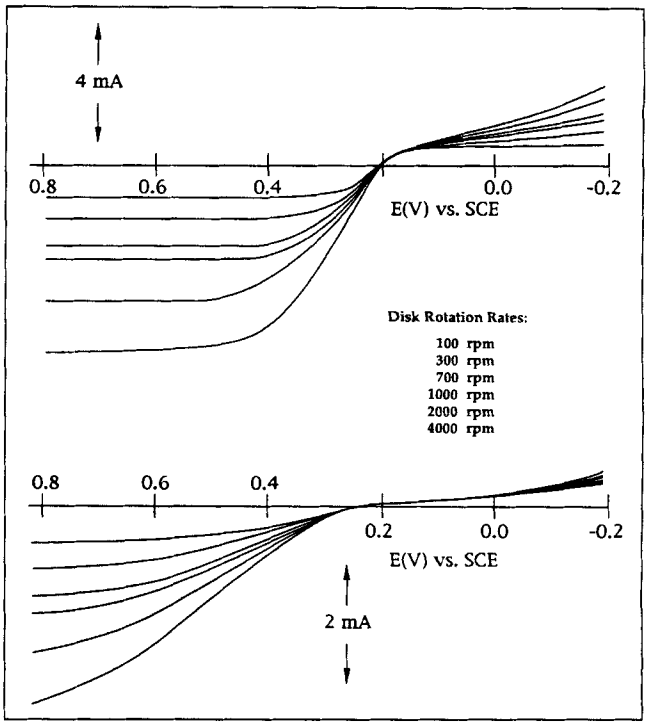

Figure 6. Rotating glassy carbon disk voltammograms for a solution containing 0.0125 M $CuCl_2$, 0.0125 M CuCl, 1.0 M KCl and 0.1 M HCl.

Rotation rates = 100, 300, 700, 1,000, 2,000 and 4,000 rpm. Top—solution saturated with Ar; bottom—solution saturated with CO.

the current scale for the voltammograms under CO is twice as sensitive as for the Ar voltammograms, it is also apparent that the kinetics of both processes are inhibited by CO.

Voltammograms similar to those in Figure 6 are obtained for solutions containing only Cu(II) or Cu(I), except that only reduction or oxidation currents, respectively, are obtained. For the Cu(II) solutions under Ar or CO, holding the Pt ring potential at +1.0 V can be used to demonstrate that for disk potentials between +0.2 and −0.2 V, reduction of Cu(II) quantitatively produces Cu(I). The magnitudes of the oxidation currents observed at the ring differ from the disk currents by exactly the collection efficiency, N. For the Cu(I) solutions, attempts to observe reduction currents at the ring at potential where Cu(I) is oxidized at the disk are complicated by deposition of copper metal on the ring at even mildly negative potentials. These experiments were, however, qualitatively consistent with chemically reversible oxidation of Cu(I) at the disk.

The low, kinetically limited currents observed for reduction of Cu(II) in this electrolyte under Ar or CO are useful for understanding why the surface area of the flow electrodes needed to be so large (34,000 cm^2 or both electrodes) and why the observed cell currents in Figure 3 deviate from the theoretical line even at moderately low flow rates. As shown in the lower half of Figure 6, the reduction rate has no dependence on rotation rate when CO is present in the solution. Since Cu(II) has very little affinity for CO, the fact that reduction currents are suppressed with respect to values ob-

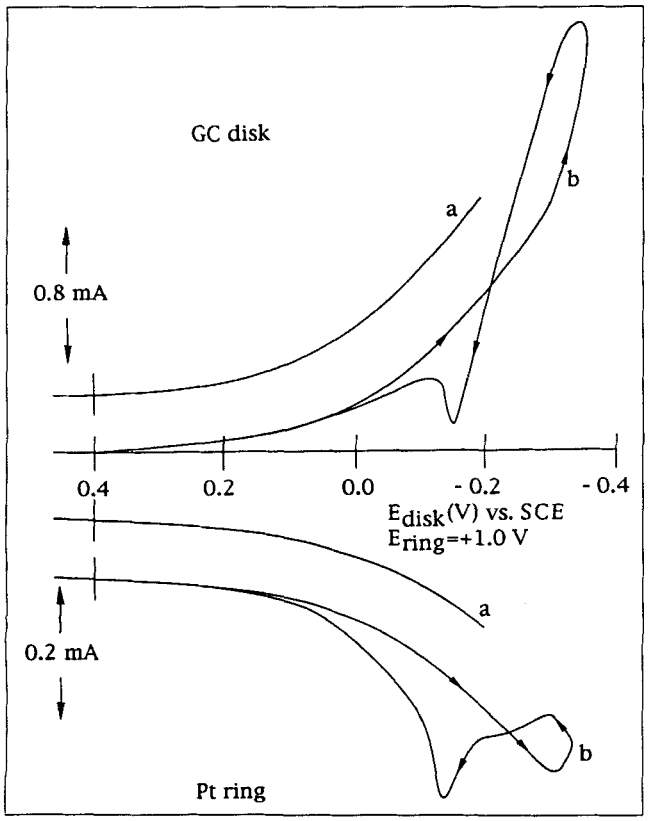

Figure 7. Rotating glassy carbon disk/platinum ring voltammogram for a solution containing 0.025 M $CuCl_2$, 1.0 M KCl, 0.1 M HCl, saturated with CO.

Rotation rate = 1,000 rpm; ring potential = + 1.0 V.

served under Ar is probably due to CO adsorption on the electrode surface. Similar rotation rate independent reduction currents are observed for the 0.025 M $CuCl_2$ solution under CO and the kinetic current density at −0.1 V (the potential applied to the cathode in the flow cells) is 1.2 mA/cm^2. This is the maximum current density that could exist at the entrance to the first flow cell at any flow rate. As the concentration of Cu(II) decreases along the solution path through the cells, the current density decreases to even lower values.

The voltammograms in Figure 6 indicate that slightly greater reduction currents could have been obtained by applying more negative potentials to the cathode. The RRDE voltammogram in Figure 7 indicates why this is not possible with this system and why three-electrode potentiostats with careful potential control of the cathode were necessary for the flow electrodes. In scan (a), the disk potential was scanned to −0.2 V and then reversed. The corresponding anodic current at the ring, which is held at +1.0 V, indicates reversible oxidation of the Cu(I) formed at the disk to Cu(II). In scan (b), the potential was scanned to −0.35 V before reversal. Several features of this second scan demonstrate why applying increasingly negative potentials to the cathode in the flow cells has deleterious effects. As the disk potential becomes negative of −0.3 V, a sharp increase in the disk current is observed. The corresponding ring current, however, begins to decrease, indicating that less Cu(I) is being formed at the disk. When the potential scan is reversed, the disk current remains high until a potential of −0.15 V is reached where a sharp feature in the anodic current direction is observed. The ring current corresponding to this feature is also anodic. All of the observations just described are consistent with deposition of Cu metal at the disk at potentials negative of −0.3 V. Once Cu(0) begins to nucleate on the surface, the rate for this process increases dramatically. Only when the disk potential becomes positive of −0.2 V does the Cu(0) reoxidize to Cu(I). The ring current initially decreases when Cu(0) is being deposited at the disk because less Cu(I) is being swept out to the ring. Later, when the Cu(0) deposit on the disk is reoxidized to Cu(I), additional anodic current is observed at the ring as this Cu(I) is oxidized to Cu(II).

It is evident from Figure 6 that oxidation of Cu(I) at glassy carbon is far more facile than the reduction of Cu(II); however, oxidation is also affected by the presence of CO. Kinetically limited currents at rotating disk electrodes are conveniently analyzed by making plots of (disk current)$^{-1}$ vs. (rotation rate)$^{-1/2}$ at various electrode potentials. Extrapolation of such plots to the y-axis result in a 0-intercept if the electrode process is mass transport limited. A nonzero intercept indicates a kinetic limitation, and the value of the intercept is the reciprocal of the kinetic current, I_k. Values of I_k are readily converted to current densities J_k through dividing by the disk surface area.

For 0.025 M CuCl solutions under Ar, reciprocal plots constructed from currents at disk potentials positive +0.5 V indicate mass transport control. The behavior for 0.025 M CuCl solutions under CO is shown in Figure 8. At potentials positive of +1.0 V, the oxidation of Cu(I) is mass transport controlled. At more negative potentials, I_k becomes smaller as the oxidation becomes kinetically limited. At +0.5 V, J_k is about 12 mA/cm^2, that is, this is the largest current density that could be observed at this concentration of Cu(I), regardless of mass transport rate. Since these currents are directly proportional to [Cu(I)], maintaining high current densities throughout the flow cells is impossible unless the potential of the anode is maintained at a relatively positive potential, which increases the power consumption.

Although it is not shown in Figure 6, sweeping the disk potential to positive of 1.4 V results in the oxidation of chloride ion to Cl_2, which exists primarily as Cl_3^- under these conditions. Since the anode is connected as the counterelectrode in the flow cells, evolution of chlorine will occur if the currents being passed at the working electrode (cathode) require a highly positive counterelectrode potential. This, in fact, does occur when electrolysis in the flow cells is initiated if the solution used to charge the cells contains entirely $CuCl_2$. Once a balance between Cu(II) and Cu(I) is established, the slow rate of reduction of Cu(II) only requires moderately positive potentials at the anode and the evolution of chlorine ceases.

The carrier/electrolyte solution in this study was chosen based on previous studies indicating that the Cu(I) form of this solution reversible absorbed CO (Smith and Quinn, 1980). The electrochemical studies described earlier show that, in terms of an EMC separation/concentration process, the carrier/electrolyte solution is far from optimal. The slow kinetics observed for the reduction of Cu(II) at glassy carbon were

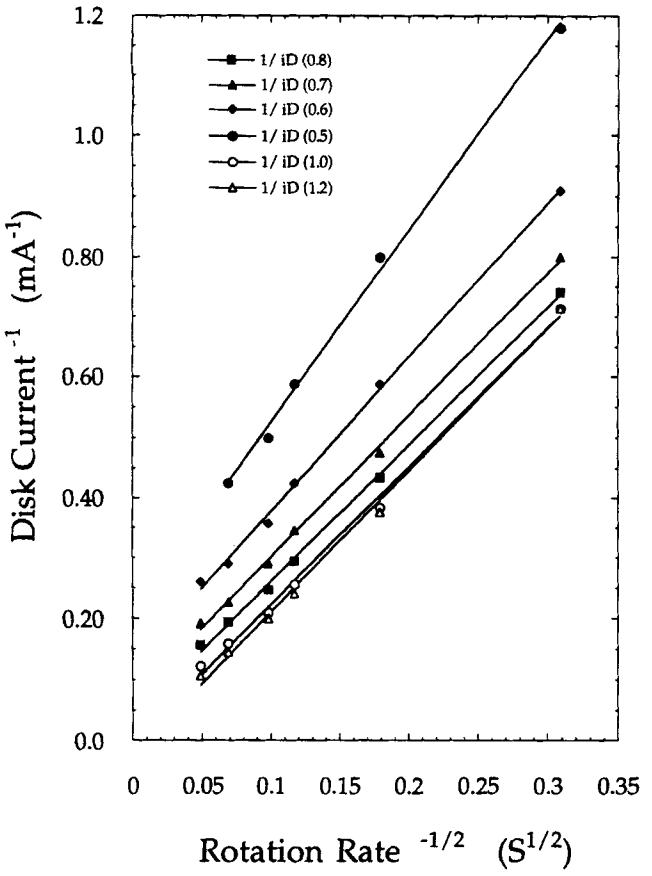

Figure 8. (Disk current) −1 vs. (rotation rate) −1/2 for the oxidation of 0.025 M CuCl, 1.0 M KCl, 0.1 M HCl, saturated with CO at a glassy carbon disk.

surprising because in previous studies (Napp et al., 1967; Miller and Bruckenstein, 1970) on the reduction of Cu(II) in 0.5 M KCl at Pt and Au electrodes reported reduction waves that were nearly mass transport limited for Cu(II)/Cu(I) and Cu(I)/Cu(0). As mentioned earlier, for the electrolyte used in this study, Cu(II) has 0, 1, or 2 coordinated chlorine ions, while Cu(I) exists as $Cu(Cl)_3^{2-}$. Possibly, this difference in coordination numbers is responsible for the slow electrode kinetics observed.

Energy requirement

Concentration of a solute requires work and/or heat energy. The minimum free energy, or work, necessary to pump a fraction of solute from a feed phase to a receiving phase follows from the chemical potential expression:

$$\Delta G = RT \ln (r/f), \tag{11}$$

where r and f are the solute concentrations of the receiving and feed phases. If the solute concentration is initially greater than that in the receiving phase, the process is spontaneous until equilibrium and no work is required. After that point, energy is required to further concentrate the solute against its concentration gradient in the receiving phase. Consequently, the minimum input work required to pump a fraction, F_r, of the initial solute present in a feed phase to a receiving phase is (Jemaa et al., 1992)

$$W_{id} = RT \ln [(V_f/V_r)(F_r/(1 - F_r))], \tag{12}$$

where V_f and V_r are the feed and receiving phase volumes, respectively.

In an EMC process this energy is supplied as electrical energy to generate the high- and low-affinity forms of the complexing agent. In this assessment, only the electrical energy for activation and deactivation of the complexing agent will be considered, that is, the energy required to pump the aqueous electrolyte phase is not included. The energy is expressed as the product of the current and potential difference between the oxidation and reduction compartments of each flow electrode:

$$W = \Sigma V \times I \tag{13}$$

where V is the applied potential and I is the current. The oxidation rate equals the reduction rate since the aqueous flow is constant and the electrode compartments are identical.

For an EMC system in which the kinetics associated with modulation of the carrier are rapid and in which one molecule of solute is absorbed for every carrier molecule in its reduced state, pumping efficiencies should be quite high (> 30%). Neither of these requirements is met in the present system; therefore, efficiencies are less than 1% for experiments like those depicted in Figure 5. The kinetic limitations on the reduction and oxidation of the carrier require relatively large applied potentials between the cathode and anode in the flow cells in order to achieve high conversions. Faster electrode kinetics for the electrolytic reactions would allow lower potentials to be used, resulting in higher energy efficiencies for the separation and concentration of CO. This may be achievable via the use of different electrolytes, alternative electrode materials, or higher temperatures. For the CO feed pressures used in this study, less than one Cu(I) complex in five binds a CO molecule; however, all carriers undergo electrolysis as they pass through the flow electrodes. A more efficient system would require use of higher pressures or a carrier with a higher affinity for CO. Identifying EMC carrier electrolyte systems for this and other gas separations with more ideal properties is the subject of our ongoing investigations.

Conclusions

An electrochemically modulated complexation process for the removal and concentration of carbon monoxide has been investigated. This process is potentially important since it offers an energy-efficient method for selectively separating and concentrating gases. A mass separating agent has been used to accomplish this purpose. It is electrochemically regenerated via flow electrodes placed in the system. A model has been developed that successfully predicts the system's behavior.

The extraction and concentration of carbon monoxide from a mixture with nitrogen has been successfully demonstrated. A difference in the partition coefficients, primarily due to

chemical solubility, between these two compounds and the Cu(I) aqueous solution allowed for the selectivity of the separation. These coefficients can be altered to improve the separation by increasing the complexing agent concentration.

The value of this process is that it introduces a novel separation technique that can potentially be applied to other gas solutes. The primary work in using the process is locating complexing agents with the required characteristics. This process can potentially be used to transport such gases as CO_2 and H_2S and selectively separate paraffins from olefins when the appropriate complexing agent is used.

Acknowledgments

This research is supported by the Center for Separations Using Thin Films (CSUTF) at the University of Colorado and a Patricia Roberts Harris Fellowship.

Notation

C_f^0 = solute concentration in feed gas phase at module entrance, M
C_f^{0*} = feed phase concentration in equilibrium with aqueous-phase concentration at module entrance, M
C_f^1 = solute concentration in feed gas phase at module exit, M
C_f^{1*} = feed-phase concentration in equilibrium with aqueous-phase concentration at module exit, M
$C_{ox}P$ = carrier-solute complex (oxidized form) concentration, M
C_r^0 = solute concentration in receiving gas phase at module entrance, M
C_r^{0*} = receiving-phase concentration in equilibrium with aqueous-phase concentration at module entrance, M
C_r^1 = solute concentration in receiving gas phase at module exit, M
C_r^{1*} = receiving-phase concentration in equilibrium with aqueous-phase concentration at module exit, M
$C_{red}P$ = carrier-solute complex (reduced form) concentration, M
G = Gibbs free energy, J/mol
m = distribution coefficient (no carrier present)
Q_a = aqueous-phase flow rate, cm^3/s
Q_f = feed-phase flow rate, cm^3/s
Q_r = receiving-phase flow rate, cm^3/s
R = ideal gas constant, J/(mol·K)
Sh = Sherwood number (k·v/D)
t = time, s
T = temperature, K
W_{id} = ideal work required, J

Literature Cited

Bard, A. J., and L. R. Faulkner, *Electrochemical Methods*, Chap. 8, Wiley, New York (1980).

Chaltykyan, O. A., "Copper-Catalytic Reactions," Consultants Bureau, New York (1966).

Dindi, A., R. D. Noble, C. A. Koval, and J. Yu, "Experimental and Modeling Studies of a Parasitic Binding Mechanism in Facilitated Membrane Transport," *J. Memb. Sci.*, **66**, 55 (1992).

Jemaa, N., R. D. Noble, and C. A. Koval, "Combined Mass and Energy Balance Model of an Electrochemically Modulated Equilibrium Stage Process," *Chem. Eng. Sci.*, **47**(6), 1469 (1992).

Jemaa, N., H. Walls, R. D. Noble, D. Wedman, and C. A. Koval, "Continuous Electrochemically Modulated Complexation SeparationsProcess," *AIChE J.*, **39**(5), 867 (1993).

McConnell, H., and N. Davidson, "Spectrophotometric Investigation of the Copper(II)-chloro Complexes in Aqueous Solution of Unit Ionic Strength," *J. Amer. Chem. Soc.*, **72**, 3164 (1950).

Miller, B., and S. Bruckenstein, "Hydrodynamic Potentiometry and Amperometry ar Ring-Disk Electrodes," *J. Electrochem. Soc.*, **117**, 1032 (1970).

Napp, D. T., D. C. Johnson, and S. Bruckenstein, "Simultaneous and Independent Potentiostatic Control of Two Indicator Electrodes," *Anal. Chem.*, **39**, 481 (1967).

National Research Council, *Separations and Purification: Critical Needs and Opportunities*, National Academy Press, Washington, DC (1987).

Prasad, R., and K. Sirkar, "Solvent Extraction with Microporous Hydrophilic and Composite Membranes," *AIChE J.*, **33**(7), 1057 (1987).

Smith, D. R., and J. A. Quinn, "The Facilitated Transport of Carbon Monoxide Through Cuprous Chloride Solutions," *AIChE J.*, **26**, 112 (1980).

Ward, W. J., "Analytical and Experimental Studies of Facilitated Transport," *AIChE J.*, **16**, 405 (1970).

Winneck, J., "Electrochemical Membrane Gas Separation," *Chem. Eng. Prog.*, 41 (1990).

Manuscript received Oct. 21, 1994, and revision received Jan. 23, 1995.